JOURNAL OF CATALYSIS 84, 333–343 (1983)

EXAFS Studies of Pt/Al_2O_3 Catalysts

P. LAGARDE,* T. MURATA,*,[1] G. VLAIC,*,[2] E. FREUND, H. DEXPERT,
AND J. P. BOURNONVILLE

*Laboratoire pour l'Utilisation du Rayonnement Electromagnétique (LURE), Bâtiment 209 C, Université Paris-Sud, 91405 Orsay, and Institut Français du Pétrole, B.P. 311, 92506 Rueil-Cédex, France

Received January 17, 1983; revised June 1, 1983

Industrial Pt/Al_2O_3 catalysts have been studied by EXAFS (extended x-ray absorption fine structure) at various stages of preparation from the dried impregnated support to the reduced catalyst. The structure of the environment of the metal starts from $PtCl_6$ units. After calcination at 530°C, Exafs gives evidence for a Pt–O interaction coming either from small oxide particles or from bonds with oxygen atoms of the carrier surface. Large metal aggregates grow with higher calcination temperatures (up to 700°C in this work), in agreement with electron microscopy results. On cubic gamma-alumina (γ_c-Al_2O_3) the clusters obtained by H_2 reduction are suggested to be cubo-octahedral units of about 13 atoms in the fcc structure. Moreover, Exafs shows some evidence for metal–support interaction.

INTRODUCTION

Extended X-ray absorption fine structure (EXAFS) is proving to be a valuable tool for studying highly dispersed supported metallic catalysts. The results already published (*1–3*) clearly demonstrate that this technique allows a determination of the local structural parameters (interatomic distances R, coordination numbers N) which are difficult to measure by any other method because of the very high dispersion state of the system.

In this paper we report Exafs results obtained on the L_{III} edge of the metal for alumina-supported platinum catalysts of the same type as those used for naphtha reforming in the petroleum industry. No platinum crystallites larger than 10 Å can be observed by high-resolution electron microscopy and the platinum content (0.2–0.6% wt in the industrial catalysts) is very low. In order to understand the impregnation process, usually carried out with hexachloroplatinic acid solution, we also studied a catalyst prepared using hexabromoplatinic acid: in this case the *K*-edge Exafs of bromine can be obtained and compared to the platinum results while the chlorine one is not available.

The catalyst has been studied during the various stages of its preparation and using different types of alumina. We shall show that the local environment and the chemical state of a platinum atom depend on the physicochemical treatment of the catalyst, and that the bulk and surface structure of the support influences the final state of the metal after the reduction process.

EXPERIMENTAL

A. Methods. The catalysts were 1.5 wt% platinum supported on γ-alumina extrudates (BET surface area: 240 m^2/g). Platinum was impregnated in hydrochloric and hydrobromic acid aqueous solutions according to the nature of the metallic precursor used, i.e., hexachloroplatinic and hexabromoplatinic acid. Platinum and halogen contents were determined by X-ray fluorescence. The metallic surface area was measured by classical hydrogen–oxygen titration (*4*) and checked by electron micros-

---

[1] Present address: Kyoto University of Education, 1-Fukasuka, Fujinomoni-cho, Fushimi-ku, Kyoto 612, Japan.

[2] Present address: Istituto Donegani, Via Fauser 4, 28100 Novara, Italy.

0021-9517/83 $3.00

copy. In the case of γ_c-alumina the chemisorption measurements gave dispersions of 0.80 and 0.84 for the reduced samples previously calcined at 530°C (for the chlorine and the bromine impregnation, respectively). These values correspond to particles with diameters close to 10 Å. For the samples previously calcined at 700°C the dispersion dropped to 0.04 for the hydrochloric precursor and to 0.2 for the hydrobromic one, numbers characteristic of much larger particles (100 Å and more).

The experiments were carried out on the Exafs I spectrometer at LURE-DCI, using a silicon (220) channel-cut monochromator, the ring running typically at 1.72 GeV, 250 mA.

For the liquid reference compounds (hexachloro- and hexabromoplatinic acid solutions) the sample holder was a cell with Mylar windows, identical to that described in a study of electrolytic solutions (*5*) while the apparatus used for solid samples was a furnace with boron nitride holders designed by Lytle *et al.* (*1*). This apparatus allows an *in situ* treatment (calcination and reduction) of the catalyst without any contact with the atmosphere, the same sample being used for all the steps. In all cases (catalysts as well as reference compounds) Exafs spectra have been taken at room temperature.

B. Data analysis. All Exafs spectra have been analyzed using a now well-known data processing procedure. The pre-edge absorption coefficient is first fitted with a Victoreen expression which is extrapolated to the energies after the edge; the atomic absorption is approximated first with a second-degree polynomial and the remaining long-wavelength oscillations on the Exafs due to errors in this second-order polynomial fit are removed by a multi-iteration curve smoothing, the effect of which is carefully checked. It must appear only in the very low R values in the modulus of the Fourier transform (FT)—typically $R < 1$ Å—where interatomic distances are physically unreasonable. Before Fourier transforming a window has to be applied to the data: we chose the Hanning function and in all cases subject to comparison (for instance elemental foil and reduced samples) the same window function has been used in order to keep identical all the spurious mathematical ripples due to the filtering.

When a backtransformed contribution of one given shell has been analyzed through the classical Exafs formula the theoretical phase shifts used were those from Teo and Lee (*6*). It should be noted that the backscattering quantities for platinum have a strong valley in the range 100 to 150 eV. The accuracy of the calculations of the phase shifts in this domain is not perfect and the effect on the Fourier transform of this rapidly changing phase is very large, causing the splitting of the first shell on the magnitude of the Fourier transform of Pt metal. This induces a quite large discrepancy between experimental and theoretical curves in the corresponding domain. Since the Exafs data due to platinum extend to high energies (up to 800 eV) this misfit is not of importance in analyzing the Pt–Pt contributions; nevertheless, we slightly corrected the corresponding electronic quantities, and we used the corrected backscattering amplitude and phase in all the analysis. For completeness, in order to label the numerical parameters entering the tables, we recall here the Exafs formula and the notations used:

$$\chi(E) = -\sum_j \frac{N_j}{kR_j^2} e^{-2\sigma_j^2 k^2} e^{-\Gamma_j R_j/k} |f_j(\pi)| \sin(2kR_j + \phi_j) \quad (1)$$

$$\phi_j = 2\delta_1' + \psi_j(k)$$

where δ_1', ψ_j, and $|f_j|$ are, respectively, the central atom phase shift, the phase, and the amplitude of the backscattering, σ is the Debye-Waller like factor, and Γ is related to the mean free path of the photoelectron.

In all the analysis on Pt, the edge has been fixed at 11,560 eV and the tables indicate the shift used, starting from this value, of the experimental origin of the energies in the corresponding fits versus the calculated

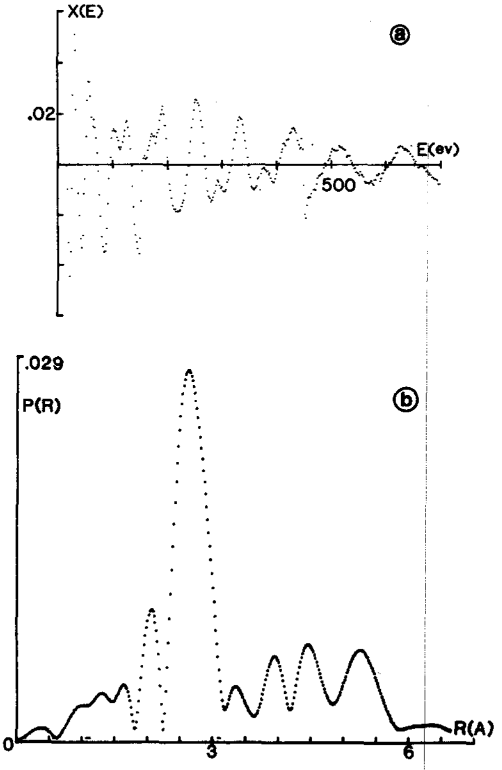

FIG. 1. (a) Experimental Exafs data for a 15-μm platinum foil. (b) Amplitude of the Fourier transform of Pt metal ($k^3 \cdot X(k)$). The Hanning window used has the following limits: 50–70, 650–720 eV.

ones. For instance, a ΔE^0 of +10 eV means that the energy of the edge has been taken in the experimental data at 11,570 eV. In case of Br, E^0 has been fixed at 13,475 eV.

RESULTS AND DISCUSSION

Model Compounds

Different model compounds have been used to check, as usual, the electronic parameters such as phase shifts and energy edge variations. We therefore analyzed elemental platinum, solutions of hexacholoroplatinic and hexabromoplatinic acids used for impregnation of the support, and platinum oxide powder as a reference for calcined samples.

In the case of the metal foil the four first shells have been analyzed separately. Figure 1a gives the raw Exafs data of a 15-μm elemental platinum foil taken at room temperature and Fig. 1b the magnitude of the Fourier transform of $k^3X(k)$ taken in a k domain spanning from 3.9 to 13.5 Å^{-1}. Figure 2 is the fit of the filtered first shell using the Exafs formula (*1*), the limits of the square window used in the R space being 1.8 and 3.18 Å.

Table 1 shows the numerical values entering into the different fits and the following features can be pointed out. While the first shell is quite well fitted with the crystallographic value of R = 2.76 Å, the agreement for the outer shells is less accurate. This general feature of Exafs analysis, at least in the case where we intend to keep constant the electronic parameters from one shell to another, is not of great impor-

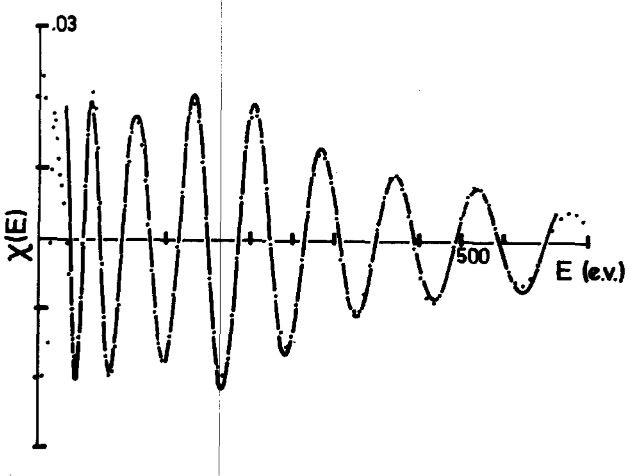

FIG. 2. Fit of the backtransformed first shell of Fig. 1b using the parameters listed in Table 1.

TABLE 1

Exafs Parameters Used for the Fits of the Model Compounds

Compound	Neighbor	R (± 0.02 Å)	N (± 0.5)	σ (± 0.002 Å)	Γ (± 0.07 Å^{-2})	E° (± 2 eV)
Pt metal	Pt	2.76	12	0.068	2.50	11,560
Pt oxide	O	2.04	6	0.068	2.40	11,580
	Pt	3.10	4	0.074	2.50	11,580
		3.35	8	0.074	2.50	11,580
H_2PtCl_6	Cl	2.32	6	0.053	1.96	11,572
H_2PtBr_6	Br	2.45	6	0.042	1.96	11,560
H_2PtBr_6	Pt	2.45	1	0.058	2.14	13,467
Br edge	Br	3.46	4	0.084	2.14	13,467

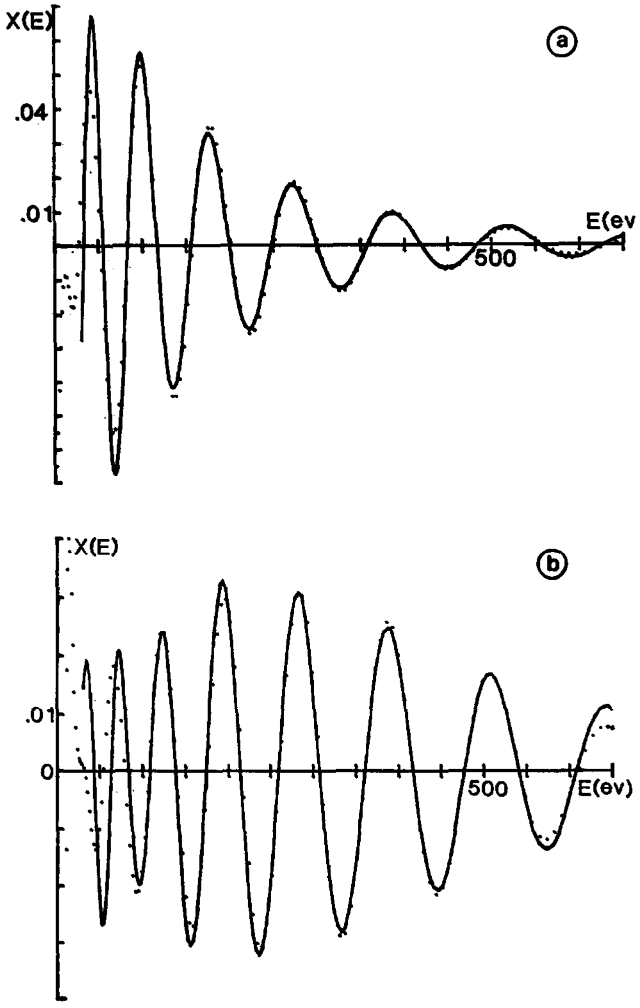

FIG. 3. (a) Fit of the backtransformed first shell of H_2PtCl_6 using parameters of Table 1. The window is the same as that in Fig. 1b. (b) Fit of the backtransformed first shell of H_2PtBr_6 on the Pt edge.

tance insofar as we are going to compare data processed in exactly the same way. Moreover, the effect of multiple scattering by the first shell on the behavior of the fourth one in fcc structures is well established (*7*).

Similar comments need to be made also on the analysis of the solutions H_2PtCl_6 and H_2PtBr_6; no crystallographic data were available but the Exafs result leads to a very accurate value of 2.32 Å for the Pt to Cl distance, while the Pt–Br distance is equal to 2.45 Å as can be seen from the quality of the fits of the first shells (Fig. 3). On this latter compound a check can be made by looking at the bromine edge. The useful range of energy in this case is not very wide, due to the L_I edge of the platinum; nevertheless, the Exafs data can be fitted with the given Br–Pt distance of 2.45 Å and the calculated one for the Br–Br neighbors (3.46 Å) assuming that the molecule is octahedral, which is likely. Figure 4 shows the result obtained in that case of the bromine edge, the structural values being again listed in Table 1.

Platinum oxide is well known for having several crystallographic forms (*8*); the Fourier transform (Fig. 5) exhibits two contributions, the Pt–O distance at 2.05 Å, very close to the 2.02-Å separation for the same pair in PtO_2, and a second peak located around 3 Å. The best hypothesis for the origin of this peak is 6 Pt at 3.10 Å and 8 Pt at 3.35 Å. Although an exact modeling is difficult, possibly because of various crystallographic phases of oxide in our sample, the presence of this peak on the Fourier transform of a catalyst can be used as a fingerprint of platinum oxide, since the Pt–Pt distances involved are definitely different from those found in the elemental metal (2.76, 3.90, 4.78, and 5.52 Å).

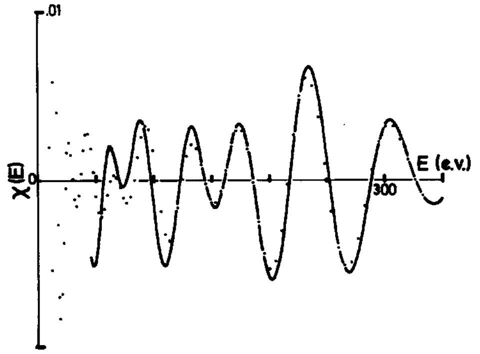

FIG. 4. Fit of the backtransformed first shell of H_2PtBr_6 on the Br edge. The parameters are listed in Table 1.

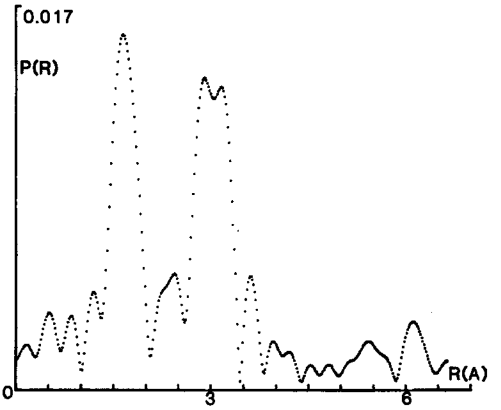

FIG. 5. Magnitude of the Fourier transform of $k^3 \cdot X(k)$ for platinum oxide. The window used is the same as in Fig. 1b.

Finally, notice also in Table 1 the different energy shifts we have used in the metal, the salt, and the oxide which are to be compared to the values entering in the analysis of the catalysts. These values of the origin of the photoelectron kinetic energy are entering the analysis of the model compounds as free parameters to obtain the correct interatomic distances, while the actual inflexion point of the different absorption edges are at the same energy (±2 eV) for all the samples. This shift is then used just in order to take into account a different chemical bonding (from ionic to metallic), which is not included in the calculations (*6*).

Impregnated and Calcined Samples

In both cases (bromine and chlorine salts) the impregnated catalysts exhibit an Exafs spectrum very close to that of the acid solution (Fig. 6); hence, as expected, the cata-

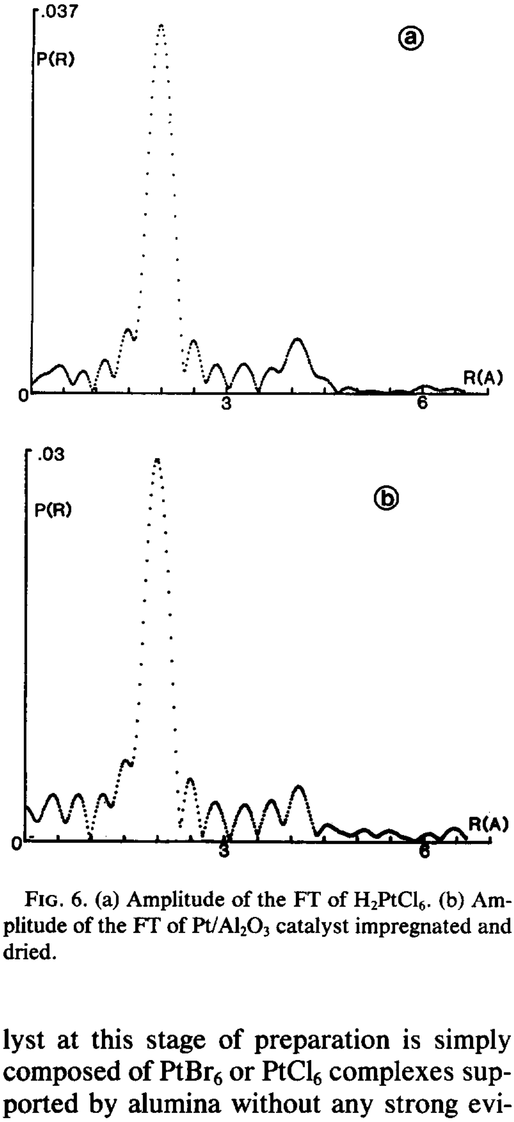

FIG. 6. (a) Amplitude of the FT of H_2PtCl_6. (b) Amplitude of the FT of Pt/Al_2O_3 catalyst impregnated and dried.

lyst at this stage of preparation is simply composed of $PtBr_6$ or $PtCl_6$ complexes supported by alumina without any strong evidence for a bonding between the metal and the support. Nevertheless, the electronic parameters listed in Table 2 show in both cases (bromine and chlorine) a slight deviation from the values used in the solution. Nevertheless, the electronic parameters listed in Table 2 show in both cases (bromine and chlorine) a slight deviation from the values used in the solution. The shift in the E° value is about 3 eV greater and the coordination number N decreases to 5.5 halogen atoms around one metal atom. Although these differences are very small and almost at the limit of the accuracy of the Exafs experiment they could be an indication for the influence of the support on the MX_6 complexes. These complexes have to be linked in some way to the alumina, but the bonding seems to be very weak and not very apparent on the Exafs spectrum.

The behavior of the samples in the calcination process (Fig. 7 and Table 3) is dependent on the temperature of the treatment and on the halogen used, but not on the duration of this heating. This last point is shown by comparing Exafs data taken for catalysts calcined at 530°C, on the same support for different times (2 or 6 h): all spectra look identical, indicating the same type of mean environment for the platinum.

Figure 7a, plotted as a function of the photoelectron energy, is the experimental result obtained in the case of the sample calcined for 2 h at 530°C. Notice the change of scale above 200 eV which allows one to see the interference phenomenon between two components of the signal. The first peak of the Fourier transform has been filtered and modeled. The result, shown in Fig. 7b, indicates clearly that the close environment of a platinum atom is not a single

TABLE 2

Exafs Parameters for the Dried Samples after Impregnation

Compound	Neighbor	R (±0.02 Å)	N (±0.5)	σ (±0.002 Å)	Γ (±0.07 $Å^{-2}$)	E° (±2 eV)
$Pt/Cl/Al_2O_3$	Cl	2.31	5.5	0.058	1.96	11,575
$Pt/Br/Al_2O_3$	Br	2.45	5.5	0.053	1.96	11,565
$Pt/Br/Al_2O_3$	Br	3.46	1.5	0.084	2.21	13,467
Br edge	Pt	2.46	0.5	0.053	2.21	13,467

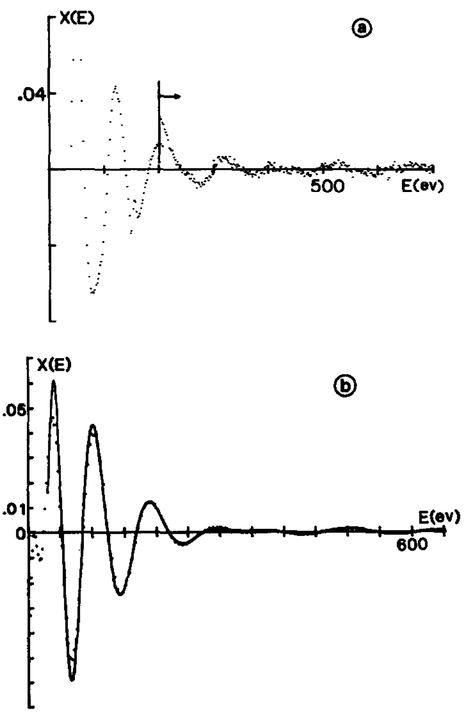

FIG. 7. (a) Experimental Exafs data of the catalyst calcined for 2 h at 530°C. Note the change of scale at 200 eV by a factor 2. (b) Fit of the backtransformed main peak of this Pt/Al$_2$O$_3$ catalyst calcined at 530°C. The parameters obtained are in Table 3 and the window used is the same as in Fig. 1b.

shell of one element. On the contrary, the mean environment of a Pt atom as given by Exafs is made up by 5 oxygen atoms at 2.01 Å, very close to the Pt-O distance in the oxide, and also by 2.5 Cl atoms at 2.32 Å, indicating that not all the chlorine has been removed by calcination. Moreover, as can be seen by comparing the two Fourier transforms (Fig. 8), the wide peak in the range 3–3.5 Å is strongly reminiscent of the large peak at the same distance seen in the FT of PtO$_2$ which we have interpreted as Pt–Pt bonds in the oxide. Thus it is reasonable to think that the metal atoms are not only bound to the support, but also that they form with the oxygen clusters of PtO$_2$, while some metal atoms still have chlorine from the impregnating solution bound to them. However, Exafs cannot give more than an average description of the situation at this stage.

The behavior on calcination of catalysts with bromine is different: we found that after the impregnation process the extraction rate of bromine by heating is higher than in the chlorine case. At the same temperature of treatment (530°C), besides the Pt-Br and the Pt–O bondings there is no longer any evidence for the peak at 3 Å found in PtO$_2$ and in the Pt/Cl catalyst (Fig. 8). Now, if the structural situation for the metal on these calcined samples was just a phase separation between Pt oxide and Pt bound to halogen, we would not expect any difference in the behavior of these distances

TABLE 3

Exafs Parameters for the Calcined Samples

Compound	Neighbor	R (±0.02 Å)	N (±0.5)	σ (±0.002 Å)	Γ (±0.07 Å^{-2})	E^0 (±2 eV)
Pt/Cl/Al$_2$O$_3$ (530°C)	O	2.01	5	0.061	2.40	11,576
	Cl	2.32	2.5	0.061	2.40	
	Pt	3.10				
	Pt	3.35				
Pt/Br/Al$_2$O$_3$ (530°C)	O	2.04	6	0.074	2.50	11,577
	Br	2.43	1	0.053	2.50	
Br edge	Pt	2.47	1	0.063	2.21	13,465
Pt/Cl/Al$_2$O$_3$ (700°C)	Pt	2.76	12	0.068	2.50	11,560
Pt/Br/Al$_2$O$_3$ (700°C)	Pt	2.76	9	0.068	2.50	11,560

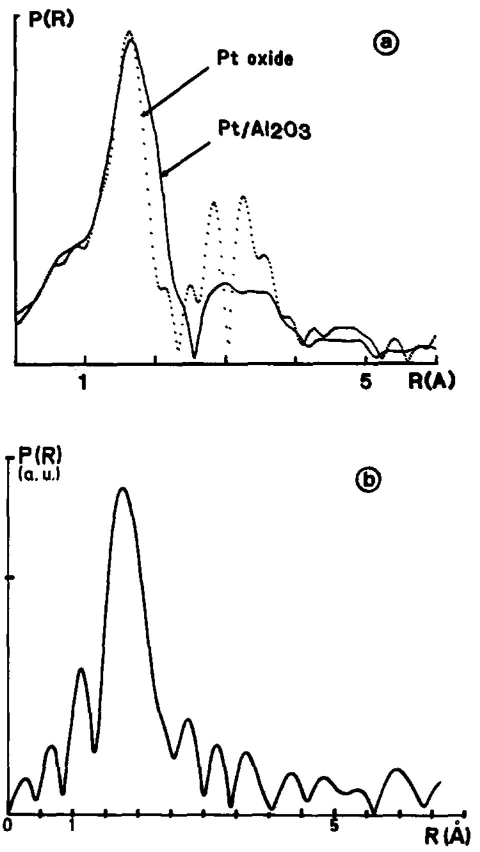

FIG. 8. (a) Amplitudes of the FT of the platinum oxide and the calcined catalyst with the same data processing showing the presence of oxide in the catalyst. (b) Amplitude of the FT of the Pt/Al_2O_3 catalyst prepared with H_2PtBr_6 after a calcination at 530°C (compare with Fig. 8a).

around 3 Å in going from Cl to Br. In effect the Pt oxide units would remain the same, at the same temperature, whatever the halogen used for the impregnation. On the contrary, the different stability of the halogen induces a change in the Pt–Pt bonding, indicating that each metal atom is at the same time bound to the halogen and to the oxygen.

On calcination at 700°C, a drastic change in the structural properties of the metal is induced, as the Exafs data of Fig. 9a show. Either on the Exafs spectrum or on the magnitude of the FT it can be seen that the chloride catalysts exhibit a structure very close to that of the metal; in particular the first neighbor distance is again 2.76 Å and each Pt atom is surrounded by 12 neighbors (Table 3). It is therefore easy to conclude that the metal atoms are gathered in quite large clusters: on the magnitude of the FT the outer shells are at the same position and have almost the correct amplitude compared to the equivalent analysis in the elemental foil. Formation of platinum metal is in agreement with the thermodynamic instability of PtO_2, which decomposes to metal above 600°C.

By contrast the behavior of the bromine system is slightly different and seems to keep a certain degree of memory of the former treatment. On calcination at 700°C the metal is more finely divided and the size

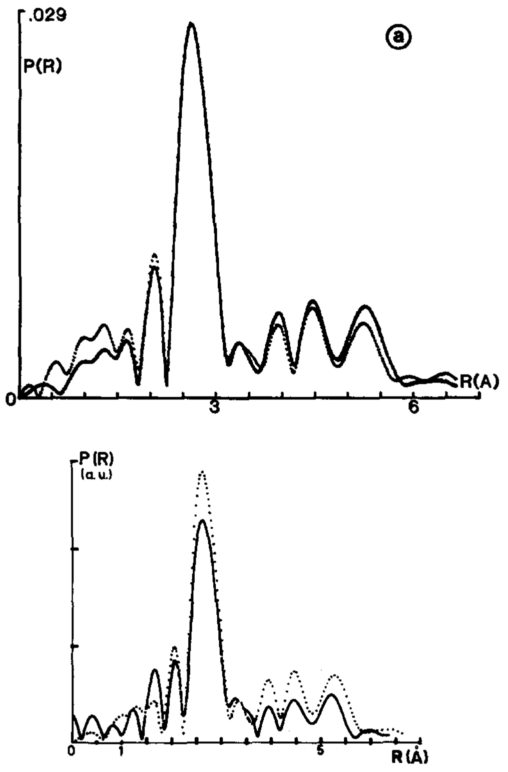

FIG. 9. (a) Amplitudes of the FT of Pt metal (solid line) and of the Pt/Al_2O_3 catalyst (dots) prepared with the H_2PtCl_6 solution and calcined at 700°C. (b) Amplitudes of the FT of Pt metal (solid line) and of the Pt/Al_2O_3 catalyst (dots) prepared with the H_2PtBr_6 solution and calcined at 700°C.

TABLE 4

Exafs Parameters for a Reduced Sample

Compound	Neighbor	R (± 0.02 Å)	N (± 0.5)	σ (± 0.002 Å)	Γ (± 0.07 Å^{-2})	E^0 (± 2 eV)
$Pt/Cl/\gamma_c$-Al_2O_3	Pt	2.75	6	0.074	2.50	11,560
	Pt	3.90	2			
	Pt	4.80	5			
	Pt	5.50	0.5			
	O	2.07	0.7	0.116	2.50	11,580

of the clusters is smaller on the average: while the distances are still the same as in the metal the reduction in amplitude indicates a first coordination number of about 8 to 9, which is the mean value for cubic clusters with an edge of about 10 Å (*9*). Since the ratio values of the second and third neighbors are identical to those of the metal it can be thought that the crystallographic configuration of these clusters is still face-centered cubic, as in the metal (Fig. 9). Table 3 summarizes all the numerical results.

Reduced Samples

We have only reduced the sample prepared with the chlorine solution, and this has been done at 480°C under hydrogen. As already pointed out, the Exafs data have been taken at room temperature, the sample holder still being under the H_2 flux and not evacuated as was done in some earlier studies (*2*).

The results obtained on the reduced sample are summarized in Table 4.

There are two main features. Although the resolution in distance measurements is of the order of 0.02 Å the first neighbor distance is measured at 2.75 Å, slightly shorter than in the elemental metal, and the coordination number is 6. These are results from a fit of the filtered first shell extracted from the experimental data shown in Fig. 10a, which has to be compared with the result on elemental platinum foil in Fig. 1a. Figure 10b shows the two Fourier transforms where it must be kept in mind that the two sets of data have been processed in exactly the same way. Since we have used in the fit almost the same Debye-Waller factor as in the metal, this reduction can hardly be attributed to an increase of the asymmetry of the distribution and appears to be reliable. Analyzing the successive shells and com-

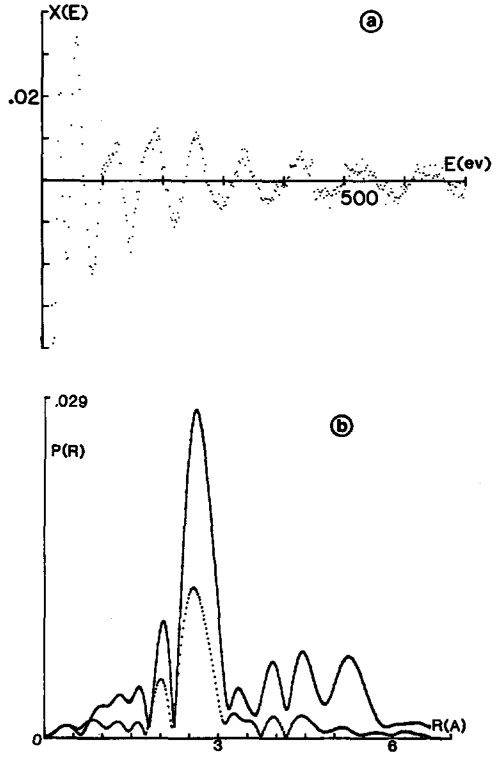

FIG. 10. (a) Experimental Exafs data on the platinum edge of the γ_c-alumina-supported catalyst reduced in H_2 at 480°C. (b) Comparison between the magnitudes of the FT of the Pt metal (solid line) and of the catalyst on γ_c-alumina (dots) reduced in H_2 at 480°C.

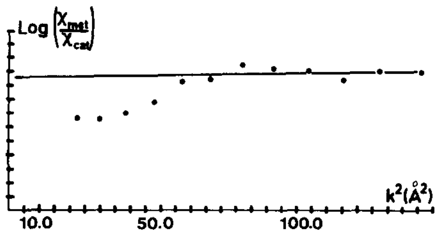

FIG. 11. Plot of the quantity log(χ(metal)/χ(cat.)) versus k^2 for the catalyst supported on γ_c-alumina and reduced in H_2.

paring with the same analysis in the metal we conclude that the coordination numbers of the 1st, 2nd, 3rd, and 4th shells are, respectively, about 6, 2, 5, and less than 0.5. While the accuracy of such a determination is quite low (about 0.5 atom) the average numbers we find here are consistent with what we would expect from a cluster of 13 atoms, a central one being surrounded by 12 neighbors in the fcc structure. Because of the well-known shadowing effect between the first and the fourth shells on this structure the information extracted from this last distance is less reliable, but it is nevertheless in line with the preceding ones. This is surprising since some theoretical calculations (*10, 11*) and experiments on platinum in zeolites (*12*) indicate that the icosahedral shape for such small particles should be energetically preferred. However, this last structure would lead to a completely different set of values for the second and third distances, and we can definitely exclude it.

Figure 11 is the plot of the quantity $\log(\chi_{met.}/\chi_{cat.})$ versus k^2 which shows two regimes: the high energy domain ($E > 250$ eV, $k > 60$ A^2) is linear and gives for σ and the coordination numbers the exact values found with the fit, while the low energy domain has a different behavior with a different slope. More reliable information is difficult to extract at this point but most probably it is evidence for metal–support interaction through a Pt–O bonding, because its backscattering function oxygen appears only in the first 300 eV and in this case its contribution should be quite large. We have tried to model it as shown in Fig. 12. The effect of 0.7 atoms of oxygen has been added to the main Pt–Pt contribution. The result shows that a definite, but not perfect, improvement can be obtained by assuming a larger Pt–O distance (2.07 + 0.02 Å) broadened by a larger Debye-Waller factor. As has been pointed out (*13*) for Pt/TiO_2 catalysts, the metal–support interaction is not very strong: the increase of the Debye-Waller term, compared to the platinum oxide, supports this conclusion. Den Otter and Dautzenberg (*16*) suggested that the metal–support interaction could be through a Pt–Al alloying, therefore with platinum to aluminum bonding. We did try to model our results in that sense: due to the poor accuracy obtained in modeling such a small signal in a limited energy domain, an alternative solution could effectively be a bonding of one aluminum for two platinum atoms at a distance of about 1.9 Å. This value is shorter than the usual Pt to Al distances in Pt–Al alloys, which are in the range 2.4 to 2.5 Å., so the platinum-to-oxygen bonding seems to be more likely. Moreover, as reported by Charcosset (*17*), numerous alloys prepared at temperatures higher than 1000°C exist between Pt and Al. The alumina used, which is of high specific area, could greatly diminish these temperatures but our experimental conditions (480°C) seem too gentle to observe the reduction of the carrier surface. As has been

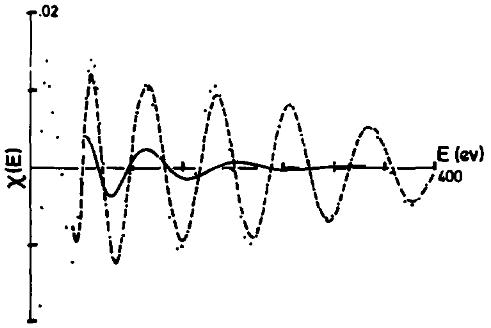

FIG. 12. Fit of the backtransformed first shell of the reduced catalyst with the parameters listed in Table 4.

shown (*16*), the alloying effect decreases the H_2 chemisorption rate and maintains or increases the O_2 one. We have never found such a behavior with the catalysts reported here.

CONCLUSIONS

By following the preparation of the catalyst from the impregnated support to the reduced sample and comparing the results with model compounds, we have been able to provide a model of the metal structure at each stage.

A substitution of bromine for chlorine changes the behavior upon calcination of the sample and Exafs confirms that the bromine compounds are thermally less stable. Calcination at 530°C induces the formation of a species between the metal and the oxygen of the support which is very similar to platinum oxide, but chlorine atoms are still present. As expected, the oxide decomposes into large clusters of metal when the calcination is done at 700°C.

On the reduced sample we believe that we have been able to extract structural information on the shape of the clusters. The best model seems to be clusters of about 13 atoms in the fcc structure of the elemental platinum metal but with some links to the support. These probable links between the active species and the support through the calcined to the reduced stage are not well characterized in this work, but more experiments are in progress using different carriers and other impregnation procedures to clarify this important point in the preparation of catalysts.

ACKNOWLEDGMENTS

We thank the Laboratoire de l'Accélerateur Linéaire for operating the DCI storage ring and for dedicated shifts.

REFERENCES

1. Sinfelt, J. H., Via, G. H., and Lytle, F. W., *J. Chem. Phys.* **76,** 2779 (1982); Lytle, F. W., Wei, P. S. P., Greegor, R. B., Via, G. H., and Sinfelt, J. H. **70,** 4849 (1979).
2. Moraweck, B., Clugnet, G., and Renouprez, A. J., *Surf. Sci. Lett.* **81,** L631 (1979).
3. Vlaic, G., Bart, J. C. J., Cavigiolo, W., and Mobilio, S., *Chem. Phys. Lett.* **76,** 453 (1980).
4. Benson, J. E., and Boudart, M., *J. Catal.* **4,** 704 (1965); Le Page, J. F., "Catalyse de Contact." Editions Technip, Paris, 1978.
5. Lagarde, P., Fontaine, A., Raoux, D., Sadoc, A., and Migliardo, P., *J. Chem. Phys.* **72,** 3061 (1980).
6. Teo, B. K., and Lee, P. A., *J. Amer. Chem. Soc.* **101,** 2815 (1979).
7. Teo, B. K., *J. Amer. Chem. Soc.* **103,** 3990 (1981).
8. Wyckoff, R. W. G., "Crystal Structures." Interscience, New York, 1965.
9. Greegor, R. B., and Lytle, F. W., *J. Catal.* **63,** 476 (1980).
10. Gordon, M. B., Cyrot-Lackmann, F., and Desjonqueres, M. C., *Surf. Sci.* **80,** 209 (1979).
11. Burton, J. J., *Catal. Rev.* **9,** 209 (1974).
12. Moraweck, B., and Renouprez, A. J., *Surf. Sci.* **106,** 35 (1981).
13. Short, D. R., Mansour, A., Cook Jr., J. W., Sayers, D. E., and Katzer, J. R., *J. Catal.* **82,** 299 (1983).
14. Sadoc, A., Raoux, D., Fontaine A., and Lagarde, P., *J. Non-Cryst. Solids* **50,** 331 (1982).
15. Marques, E. C., Sandstrom, D. R., Lytle, F. W., and Greegor, R. B., *J. Chem. Phys.* **77,** 1027 (1982).
16. Den Otter, G. J., and Dautzenberg, F. M., *J. Catal.* **53,** 116 (1978).
17. Charcosset, M., *Rev. Inst. Fr. Pet.* **34,** 969 (1979).